Alpha transfer reaction $^{16}O(^{12}C,^{8}Be_{g.s.})^{20}Ne$: Key process in the $^{12}C(^{16}O,\alpha)$ reaction

T. Murakami,* E. Ungricht,† Y.-W. Lui, Y. Mihara,‡ E. Takada,§ and R. E. Tribble
Cyclotron Institute, Texas A&M University, College Station, Texas 77843
(Received 28 May 1985)

The α-transfer reaction on ^{16}O was measured using a ^{12}C beam at 109 MeV. The reaction mechanism shows characteristics of a direct α-transfer process with a preferential high-spin population. However, the comparison with the $^{16}O(^{13}C, ^{9}Be)^{20}Ne$ reaction at 105 MeV, which was reported as a direct transfer reaction, shows large differences in the angular distributions and relative cross sections inside the same band. In order to understand those differences, both data were analyzed using the exact finite-range distorted-wave Born approximation code with the same method and parameters assuming a direct α-cluster transfer. The calculated results showed qualitative agreement with the data.

I. INTRODUCTION

Recently, we reported on the origin of prominent structures in the singles α spectrum of the $^{12}C(^{16}O,\alpha)$ reaction for incident energies of about 145 MeV.[1] In a previous publication, we had speculated that the structures were related to the direct population of known high-spin nuclear molecular states in the $^{12}C + ^{12}C$ system.[2] However, results from α-^{12}C coincidence measurements and a study of the incident energy dependence of the $^{12}C(^{16}O,\alpha)$ reaction cast considerable doubt on this explanation.[3-6] In Ref. 1, we pointed out that most of the structures observed in the singles spectra can be explained as arising from the sequential α decay of $^{20}Ne^*$ which is excited by an α pickup from the ^{12}C target. Also we noted that the target dependence of the $(^{16}O,\alpha)$ reaction[7] could be attributed to the difference of the α-pickup cross section from the target nuclei. In order to confirm this, we measured the $^{16}O(^{12}C,^{8}Be)^{20}Ne$ reaction and compared the results to those from the $^{16}O(^{13}C,^{9}Be)^{20}Ne$ reaction. The preliminary results in Ref. 1 showed that the $^{16}O(^{13}C,^{9}Be)^{20}Ne$ reaction at $E(^{13}C)=105$ MeV (Ref. 8) and the $^{16}O(^{14}N,^{10}B)^{20}Ne$ reaction at $E(^{14}N)=155$ MeV (Ref. 9) have substantially smaller cross section to high-spin states in $^{20}Ne^*$ than the $^{16}O(^{12}C,^{8}Be)^{20}Ne$ reaction at $E(^{12}C)=109$ MeV. This difference clearly supported our interpretation.

Generally the transfer reactions at an incident energy of approximately 10 MeV/nucleon are thought to be dominated by a direct mechanism. In this paper, we report the complete results of our measurement of the $^{16}O(^{12}C,^{8}Be)^{20}Ne$ reaction and compare them with the results from a measurement of the $^{16}O(^{13}C,^{9}Be)^{20}Ne$ reaction. A distorted-wave Born approximation (DWBA) analysis is presented based upon a direct α-cluster transfer reaction mechanism. Since angular distributions for the $^{16}O(^{14}N,^{10}B)^{20}Ne$ reaction are not available, this reaction was not included in the present comparison.

II. EXPERIMENTAL PROCEDURE

The measurements were performed with a 109.4 MeV $^{12}C^{3+}$ beam from the Texas A&M University 228 cm cyclotron. The incident beam energy was chosen so that the $^{12}C+^{16}O$ system would have the same center-of-mass energy as in the $^{12}C(^{16}O,\alpha)$ reaction at $E(^{16}O)=145$ MeV. A self-supporting natural Al_2O_3 foil of 150 $\mu g/cm^2$ was used as the ^{16}O target. Background from the ^{27}Al was investigated by using a 130 $\mu g/cm^2$ Al target in place of the Al_2O_3 foil. Also a 130 $\mu g/cm^2$ natural silica (SiO) target was inserted in order to confirm that none of the observed peaks were due to a Si contaminant in the Al_2O_3 target.

The outgoing ^{8}Be particles were measured by detecting the coincidence of the two α particles from the breakup using two counter telescopes consisting of 200 μm ΔE and 1.5 mm E silicon surface barrier detectors. The thickness of the ΔE detectors was chosen so that they would stop the elastically scattered ^{12}C ions. Absorber foils were not used in front of the ΔE detectors in order to preserve the energy resolution in the ^{8}Be spectra. Two telescopes collimated by circular slits were set together as close as possible in order to get a reasonably large detection efficiency. The typical full-cone angle for ^{8}Be breakup was approximately 4°. The actual separation of the telescopes was 3.4°. Both telescopes had angular acceptance of $\pm 0.9°$, which corresponds to an energy resolution of about 300 keV. The two detectors were installed perpendicular to the reaction plane in order to measure ^{8}Be events at forward angles.

The detection efficiency of our system was calculated as a function of ^{8}Be energy following Ref. 10. For our geometry we calculated that the effective solid angle ranged from 0.07 to 0.08 msr for the energies of interest. The energy calibration was obtained from elastic scattering of ^{12}C on ^{16}O and ^{27}Al targets. The calibration was then checked by comparing the calculated energies to well-known levels populated in ^{20}Ne. From this compar-

ison we estimated that the ambiguity in the energy calibration was less than ± 100 keV.

Event processing was performed with conventional electronics. Signals from each detector stack corresponding to ΔE and E, and time interval between the signals from two E detectors were recorded event by event on magnetic tape by an on-line VAX 11/780 computer and were then analyzed off-line. Data were collected at the four angles 5°, 7.5°, 10°, and 12.8°. Based upon our estimates of uncertainties in beam integration, target thickness, and solid angle, the uncertainty in the absolute cross sections was about 20%.

III. EXPERIMENTAL RESULTS

Figure 1 shows a typical ^{8}Be spectrum from the Al_2O_3 target along with a spectrum from the Al target at the same laboratory angle. The vertical scaling has been adjusted so that the peak heights in both spectra correspond to approximately the same cross section for the $^{27}Al(^{12}C,^{8}Be)$ reaction. It is clear from the data on the Al target that the $^{27}Al(^{12}C,^{8}Be)$ reaction does not contribute any distinct peaks to the spectrum from the Al_2O_3 target. Several sharp peaks are observed from the composite target which correspond to levels excited by the $^{16}O(^{12}C,^{8}Be)^{20}Ne$ reaction. Excitation energies, spins, and parities for the states identified in the figure are taken from Ref. 11. Excited states at 24.21, 25.67, and 28.1 MeV, which were observed as resonances in the elastic α scattering from an ^{16}O target[12] and from the $^{16}O(^{6}Li,d)^{20}Ne$ reaction,[13] are not visible in our spectra.

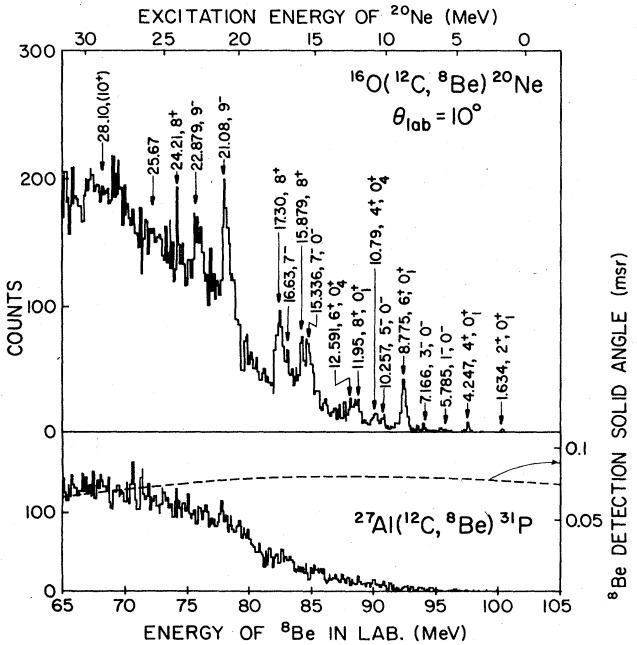

FIG. 1. Energy spectrum of ^{8}Be detected at 10°. The peaks are identified by their energies, and J^{π} and K^{π} values if previously known. The dashed curve indicates the detector efficiency as a function of the ^{8}Be energy and corresponds to the right-hand scale in the figure.

Among the more than 150 known excited states of ^{20}Ne below $E_x(^{20}Ne)=25$ MeV, the $(^{12}C,^{8}Be)$ reaction preferentially populates members of the $K^{\pi}=0_1^+$, 0^-, and 0_4^+ bands. These bands are well described in the SU(3) model by the $(\lambda\ \mu)=(8\ 0)$, $(9\ 0)$, and $(12\ 0)$ representation, respectively. Considering their structures, we would indeed expect states from these bands to be populated by a direct α-transfer reaction. States at 21.08 and 22.87 MeV which are both populated have been identified as 9^- and are candidates for the 9^- member of the 0^- band. Similarly two 8^+ states are populated at 15.88 and 17.30 MeV which are likely candidates for the 8^+ member of the 0_4^+ band. We do not observe the 5^- state at 8.45 MeV which has been reported in the $(^{6}Li,d)$ reaction at $E(^{6}Li)=75.4$ MeV,[14] the $(^{7}Li,t)$ reaction at $E(^{7}Li)=38$ MeV,[15] and the $(^{16}O,^{12}C)$ reaction at $E(^{16}O)=68$ MeV.[16] This 5^- level is a member of $K^{\pi}=2^-$ band with a 5p-1h structure and should not be populated by a direct α-transfer reaction but rather would arise from a compound or multistep process involving a 1p-1h excitation of the ^{16}O core. The absence of this state suggests that we do not have significant contributions coming from these processes. In fact, a Hauser-Feshbach calculation using the program STATIS (Ref. 17) with the parameters that were employed to analyze the $^{12}C(^{16}O,\alpha)$ reactions[1] indicates that the yield of ^{8}Be from evaporation of the compound nucleus ^{28}Si is at least two orders of magnitude smaller than the actual cross section which we observed. It is interesting to note that the population of the $K^{\pi}=0^-$ band is surprisingly large in the $(^{12}C,^{8}Be)$ reaction. Indicative of that are states at 5.79 (1^-), 7.17 (3^-), and 10.26 (5^-) MeV which are clearly populated in the $(^{12}C,^{8}Be)$ reaction but were not observed in $(^{13}C,^{9}Be)$ (Ref. 8) and $(^{14}N,^{10}B)$ (Ref. 9) reactions.

A more detailed comparison of the present $^{16}O(^{12}C,^{8}Be)^{20}Ne$ reaction and the $^{16}O(^{13}C,^{9}Be)^{20}Ne$ reaction is presented in Figs. 2 and 3. We can note several features from this comparison. First, as the excitation energy in the residual ^{20}Ne increases, the difference between the absolute cross sections of the two reactions becomes significantly enhanced. In fact, the $(^{12}C,^{8}Be)$ reaction yield to the $11.95(8^+)$ MeV state is about four times that seen in the $(^{13}C,^{9}Be)$ reaction, while the yield to the lower lying states at 1.63 (2^+) and 8.78 (6^+) MeV are comparable. Second, the angular distributions for the $(^{12}C,^{8}Be)$ reaction to high-spin states seem to be more forward peaked than those from the $(^{13}C,^{9}Be)$ reaction. This feature is very prominent in the angular distribution from the 11.95 (8^+) MeV state. Third, the population of the 22.87 (9^-) MeV state is quite weak in the $(^{13}C,^{9}Be)$ reaction in contrast to the rather strong population by the $(^{12}C,^{8}Be)$ reaction.

IV. DISCUSSION

In order to understand the differences between the $(^{12}C,^{8}Be)$ and $(^{13}C,^{9}Be)$ reactions, exact finite range DWBA calculations were carried out for the two reactions using the revised version of the code SATURN-MARS (Ref. 18) and assuming a one-step α-cluster transfer. A minor modification was made to the code since the α-transfer re-

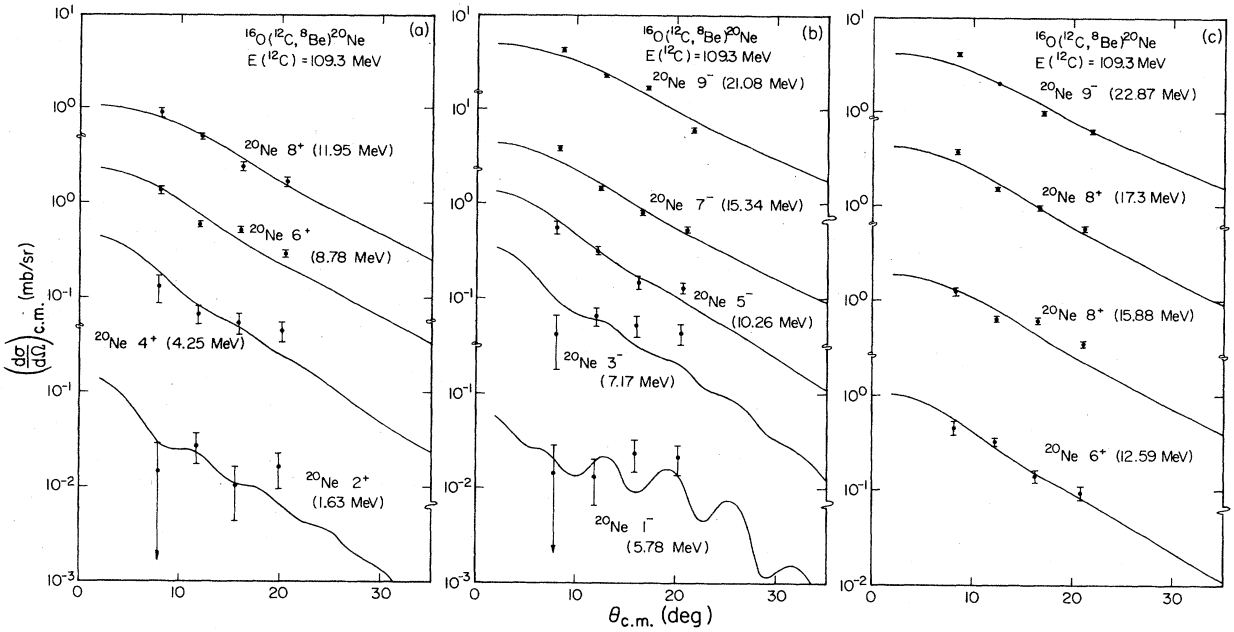

FIG. 2. The $^{16}O(^{12}C,^{8}Be)^{20}Ne$ angular distributions. The solid curves are the results of the EFR-DWBA calculation.

action is more nonlocal than the one-nucleon transfer reaction process. The post form was used consistently in the present analysis, but the Coulomb terms in the interaction[19] were not taken into account.

Most of states observed in the reactions are in the continuum since they lie above the α-decay threshold in ^{20}Ne. In the calculations that were performed, wave functions for the continuum states were replaced by bound state wave functions using a binding energy of 0.1 MeV. The appropriate experimental Q value was used for each calculation. Radial wave functions for the α-^{8}Be or α-^{9}Be and α-^{16}O systems were calculated using a Woods-Saxon potential with the parameters $R=1.2A^{1/3}$ fm, where A is the mass number of the core nucleus, and $a=0.65$ fm. The same radius was used for the Coulomb potential. The potential depth was adjusted to reproduce the binding energy of the α cluster in the α-core system. The number of nodes N for the radial wave functions was determined by the harmonic oscillator relation

$$2N+L=\sum(2n_i+l_i)\ ,$$

where L is the angular momentum of the α cluster in the projectile or final state and n_i and l_i are the number of

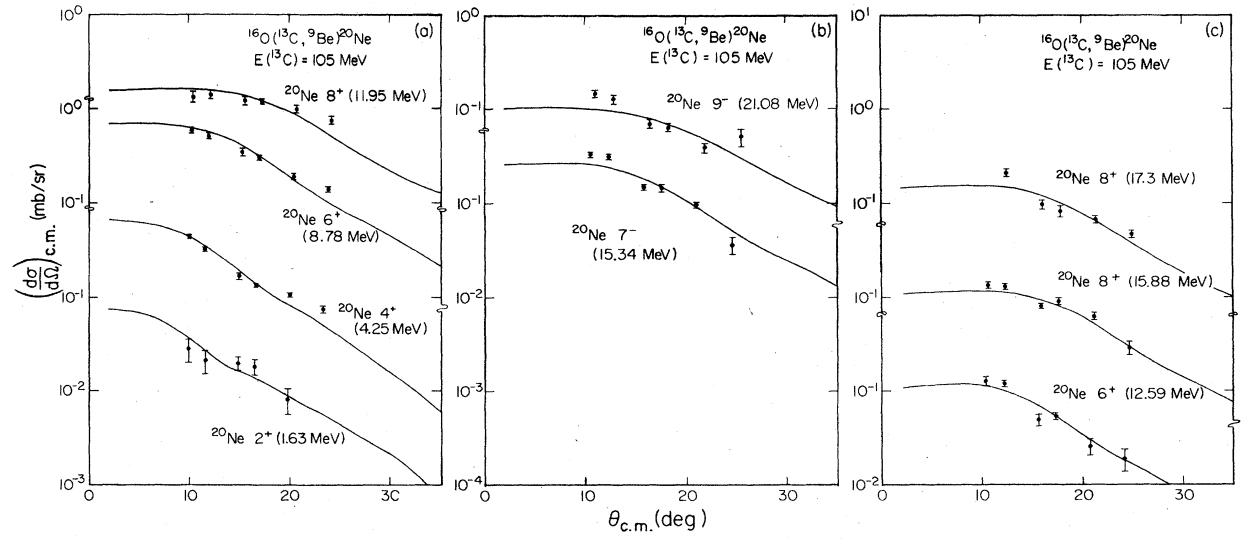

FIG. 3. The $^{16}O(^{13}C,^{9}Be)^{20}Ne$ angular distributions from Bradlow *et al.* (Ref. 8). The solid curves are the results of the EFR-DWBA calculation using the same parameter set as in Fig. 2.

TABLE I. Optical potentials used in the DWBA analysis. The form factors are Woods-Saxon type. $R = r_0(A_p^{1/3} + A_t^{1/3})$, unless r_0 is indicated as negative, in which case $R = |r_0| A_t^{1/3}$.

Channel	V (MeV)	r_R (fm)	a_R (fm)	W (MeV)	r_I (fm)	a_I (fm)	r_c (fm)
C + O	65.5	1.02	0.731	45.0	1.035	0.600	1.25
Be + Ne	190.0	−1.30	0.720	45.0	−1.300	1.200	−1.30

nodes and orbital angular momentum of the four nucleons with respect to the core, respectively. The actual values for N and L were taken from the SU(3) model; for the $K = 0_1^+$, 0^-, and 0_4^+ bands in ^{20}Ne we have $2N + L = 8$, 9, and 12, respectively, and (N,L) values for the ^{12}C and ^{13}C are (2,0) and (1,2), respectively. Since the 9^- member of the 0^- band and the 8^+ member of the 0_4^+ band have not been conclusively identified, we assumed the candidates mentioned above for these states and used the appropriate (N,L) values. With these values, we obtained α-cluster wave functions for ^{20}Ne which were quite similar to those found by Buck *et al.*, who had used the extreme cluster model with a double folding potential.[20] The positions of the nodes were well reproduced, but there was still an appreciable difference in their asymptotic behavior, particularly for the high-lying high-spin state wave functions. The optical potential parameters for calculating the distorted waves which were kept the same for both reactions were obtained from Ref. 8 and are listed in Table I. We found that the calculated cross sections varied as a function of the optical parameters in both the entrance and exit channels so that the absolute values were not reliable. Even though the relative cross sections for members within the same band are quite insensitive to the optical parameters, changes in the Woods-Saxon potential parameters used for producing radial wave functions of the α-core systems significantly affect the relative α-spectroscopic factors even within the same band. Nevertheless, using the same potential parameters and the same method for the analyses of the two reactions should allow us to determine if the DWBA formalism can account for the major differences between the two reactions.

The results of the DWBA calculations are compared with the experimental angular distributions in Figs. 2 and 3. The calculations have been normalized to the experimental results; no correction for the finite angular opening has been taken into account in the comparison. Overall the theoretical calculations do a reasonable job of accounting for the measured angular distributions. We have included in Table II values for the spectroscopic factors $S2$, for each state from the normalization factor $S1S2$ assuming Kurath's values[21] for $S1$ of 0.5567 and 0.4066 for the ^{12}C and ^{13}C ground states, respectively. As we noted above, the absolute α-spectroscopic factors are not reliable because of the variation in the predicted cross section with optical model parameters, while the ratios of spectroscopic factors in the Table II are rather insensitive to those parameters.

If both reactions are dominated by a direct α-cluster transfer which can be described by the DWBA calculations, the ratio of the α-spectroscopic factors to the same state should be equal to unity. From the results given in the Table II, it is clear that the ratios are close to unity for the low lying states, but they gradually deviate from unity as the excitation energy increases. This deviation might be partially coming from the poor description of the α-cluster wave function for the highly excited state, which we mentioned before. Indeed if we use a Woods-Saxon potential with the parameters $R = 1.2A^{1/3}$ fm and $a = 1.1$ fm, which can produce a slightly better wave function at the asymptotic region for the 7^- state, the ratios of the α-spectroscopic factors to the 7^- and 9^- states are im-

TABLE II. Spectroscopic factors for the states of ^{20}Ne.

E_x	J^π	$(^{12}C,^{8}Be)$ A	$(^{13}C,^{9}Be)$ B	Ratio A/B
1.63	2^+	0.44	0.31	1.42
4.25	4^+	0.18	0.50	0.36
8.78	6^+	0.69	0.75	0.92
11.95	8^+	1.59	0.97	1.64
5.78	1^-	1.46		
7.17	3^-	0.36		
10.26	5^-	0.27		
15.34	7^-	1.17	0.55	2.13
21.08	9^-	8.56	1.38	6.20
22.87	9^-	7.76		
12.59	6^+	0.09	0.07	1.23
15.88	8^+	0.23	0.10	2.34
17.30	8^+	0.53	0.15	3.52

proved about 10%. Clearly it is desirable to carry out the DWBA calculation using a realistic and microscopic α wave function. It should be noted that the present DWBA calculation predicts that the (^{12}C,^{8}Be) reaction to the 9^- state has about six times larger cross section than the (^{13}C,^{9}Be) reaction to the 9^- state at $\theta_{c.m.}=10°$, though this value is still not enough to explain the actual difference. Overall the DWBA formalism seems to work reasonably well in predicting the differences between the two reactions. However, it is not clear why the (^{13}C,^{9}Be) reaction does not populate the 9^- state at $E_x=22.87$ MeV. In a recent compilation,[22] this state was identified as a member of the $K^\pi=0^-$ band. Based upon this assignment, the DWBA calculations suggest that the cross section to the 9^- state should be comparable to the cross section to the 7^- state at $E_x=15.34$ MeV for both (^{12}C,^{8}Be) and (^{13}C,^{9}Be) reactions. Further investigations appear to be required to resolve this puzzle.

V. SUMMARY

The ^{16}O(^{12}C,^{18}Be)^{20}Ne reaction has been studied at an incident energy of $E(^{12}\text{C})=109$ MeV. The experimental angular distributions have been compared to exact finite range distorted-wave Born approximation (EFR-DWBA) calculations. The calculations reproduced quite well the general features observed in the data. The ambiguity in the calculations due to the variation in predicted cross section from different optical model parameters precluded us from extracting reliable α-spectroscopic factors for high-spin members of the rotational bands in ^{20}Ne. The present reaction showed more than a factor of 5 enhancement in cross section over the ^{16}O(^{13}C,^{9}Be)^{20}Ne reaction at $E(^{13}\text{C})=105$ MeV for states in ^{20}Ne above $E_x=15$ MeV. EFR-DWBA calculations reproduced the angular distributions from the (^{13}C,^{9}Be) reaction quite well and also accounted for the difference in cross section between the two reactions qualitatively.

Most of the states in ^{20}Ne* that are strongly populated by the α-transfer reactions have nearly 100% branching ratios for decay into $^{16}\text{O}+\alpha$.[23] Hence the difference in cross section for the ^{12}C- vs ^{13}C-induced reactions helps to explain the fact that the structures observed in the ^{12}C(^{16}O,α) reaction were not seen in ^{13}C(^{16}O,α) as reported in Ref. 1. Finally we note that the results from a measurement of the ^{12}C(^{16}O,α^{16}O)^{8}Be reaction[5] shows the same excited states in ^{20}Ne that we observed in the present reaction.

ACKNOWLEDGMENTS

We wish to thank Dr. T. Izumoto and the late Professor K. Nagatani for useful discussions and continuous encouragement. This work was supported in part by the U.S. Department of Energy and the Robert A. Welch Foundation. One of the authors (E.T.) was supported by the Japan-U.S. collaboration program of the Institute of Physical and Chemical Research, Wako-shi, Japan.

*Present address: Nuclear Physics Laboratory, University of Washington, Seattle, WA 98195.

†Present address: Institut für Mittelenergie Physik, SIN, Villigen, Switzerland.

‡Permanent address: Department of Physics, Tokyo Institute of Technology, Tokyo 152, Japan.

§Present address: Department of Physics, University of Tokyo, Tokyo 113, Japan.

[1] T. Murakami, E. Ungricht, N. Takahashi, Y.-W. Lui, Y. Mihara, R. E. Neese, E. Takada, D. M. Tanner, R. E. Tribble, and K. Nagatani, Phys. Lett. **120B**, 319 (1983); Phys. Rev. C **29**, 847 (1984).

[2] K. Nagatani, T. Shimoda, D. Tanner, R. Tribble, and T. Yamaya, Phys. Rev. Lett. **43**, 1480 (1979).

[3] W. D. Rae, R. G. Stokstad, B. G. Harvey, A. Dacal, R. Legrain, J. Mahoney, M. J. Murphy, and T. J. M. Symons, Phys. Rev. Lett. **45**, 884 (1980).

[4] J. S. Karp, D. Abriola, R. L. McGrath, and W. A. Watson III, Phys. Rev. C **27**, 2649 (1983).

[5] T. Shimoda, S. Shimoura, T. Fukuda, M. Tanaka, H. Ogata, I. Miura, E. Takada, M.-K. Tanaka, K. Takimoto, and K. Katori, J. Phys. G **9**, L199 (1983).

[6] P. M. Stwertka, T. M. Cormier, M. Herman, N. Nicolas, A. Szanto de Toledo, M. M. Coimbra, and N. Carlin Filho, Phys. Rev. Lett. **49**, 640 (1982).

[7] N. Takahashi, T. Yamaya, R. Tribble, E. Takada, Y.-W. Liu, D. Tanner, and K. Nagatani, Phys. Lett. **108B**, 177 (1982).

[8] H. S. Bradlow, W. D. M. Rae, P. S. Fisher, N. S. Godwin, G. Proudfoot, and D. Sinclair, Nucl. Phys. **A314**, 171 (1979).

[9] K. Nagatani, C. W. Towsley, K. G. Nair, R. Hanus, M. Hamm, and D. Strottman, Phys. Rev. C **14**, 2133 (1976).

[10] R. E. Brown, J. S. Blair, D. Bodansky, N. Cue, and C. D. Kavaloski, Phys. Rev. **138**, B1394 (1965).

[11] F. Ajzenberg-Selove, Nucl. Phys. **A300**, 1 (1978).

[12] C. Bergman and R. K. Hobbie, Phys. Rev. C **3**, 1729 (1971).

[13] K. P. Artemow, V. Z. Gol'dberg, I. P. Petrov, V. P. Rudakov, I. N. Serikov, and V. A. Timofeev, Yad. Fiz. **23**, 489 (1976) [Sov. J. Nucl. Phys. **23**, 257 (1976)].

[14] T. Tanabe, M. Yasue, K. Sato, K. Ogino, Y. Kadota, Y. Taniguchi, K. Obori, K. Makino, and M. Tochi, Phys. Rev. C **24**, 2556 (1981).

[15] M. E. Cobern, D. J. Pisano, and P. D. Parker, Phys. Rev. C **14**, 491 (1976).

[16] F. Pougheon, P. Roussel, M. Bernas, F. Diaf, B. Fabbro, F. Naulin, E. Plagnol, and G. Rotbard, Nucl. Phys. **A325**, 481 (1979).

[17] R. Stokstad, Yale University Wright Nuclear Structure Laboratory, Internal Report 52, 1972 (unpublished).

[18] T. Tamura and K. S. Low, Comput. Phys. Commun. **8**, 349 (1974); T. Tamura, T. Udagawa, K. E. Wood, and H. Amakawa, *ibid.* **18**, 163 (1979).

[19] R. M. DeVries, Phys. Rev. C **11**, 2105 (1975).

[20] B. Buck, C. B. Dover, and J. P. Vary, Phys. Rev. C **11**, 1803 (1975).

[21] D. Kurath, Phys. Rev. C **7**, 1390 (1973).

[22] F. Ajzenberg-Selove, Nucl. Phys. **A392**, 1 (1983).

[23] S. J. Sanders, L. M. Martz, and P. D. Parker, Phys. Rev. C **20**, 1743 (1979).